NANO LETTERS

2008
Vol. 8, No. 4
1120-1126

Stochastic Modulation in Molecular Electronic Transport Junctions: Molecular Dynamics Coupled with Charge Transport Calculations

David Q. Andrews,* Richard P. Van Duyne, and Mark A. Ratner

Northwestern University, 2145 Sheridan Road, Evanston, Illinois 60208

Received December 13, 2007; Revised Manuscript Received February 16, 2008

ABSTRACT

The experimental variation in conductance that can be expected through dynamically evolving Au−molecule−Au junctions is approximated using molecular dynamics to model thermal fluctuations and a nonequilibrium Green's function code (Hückel-IV 2.0) to calculate the charge transport. This generates a statistical set of conductance data that can be used to compare directly with experimental results. Experimental measurements on Au−single molecule junctions show a large variation in conductance values between different identically prepared junctions. Our computational results indicate that the Au−Au and the Au−molecule fluctuations provide extensive geometric freedom and an associated broad distribution in calculated conductance values. Our results show agreement with experimental measurements of the low bias voltage conductance and conductance distribution for both thiol−Au and amine−Au linker structures.[1–3]

The experimental realization of single molecule transport junctions is a very exciting step in the development of miniature electronic components. The potential to use single molecules as discrete electronic devices is one driving force in molecular electronics research.[4] The other is the challenge of understanding how charge is carried in nonequilbrium metal/molecule electrode structures. Transport at the single molecule level requires fine control at the atomic scale, which is currently difficult experimentally. The fundamental question driving our research is what variation in current can be expected from the simplest of molecular devices in an ideal situation. Specifically what is the variation in current due to thermal fluctuations of a molecule between two well-defined Au electrodes separated a fixed distance? Also, can this calculation methodology be used to model experimental measurements? The variation in conductance is extremely relevant as recent computational efforts have postulated that a sulfonated vinylbenzene could be used as a miniature molecular switch[5] or as a quantum interference effect transistor.[6]

A few initial measurements on transport through single molecule junctions have been made, but there is uncertainty about the structure and dynamics within the measured junction. To date, the majority of single molecule experiments have used either a scanning probe technique to make contact to the molecule[7] or the related technique of mechanically controlled break junctions. There are also a number of other test beds, usually involving molecules in a self-assembled monolayers.[8–10] The benefit of using scanning probe techniques is the ability to create a statistically significant number of molecular junctions in solvent or under ultrahigh vacuum (UHV) conditions.[3,11–13] The one characteristic that defines all of these experiments is the lack of independent verification of the contact electrode structure and molecular geometry within the device.

The ability to make a large number of molecular junctions was first shown using a mixed monolayer containing thiol- and dithiol-terminated molecules. Au clusters were then deposited on the surface, sticking only to the molecules with thiol termination exposed. An atomic force microscope probe could then image the surface and record conductance values at each location.[7] A histogram of over 4000 such traces using octanethiol/octanedithiol molecules showed peaks at integer multiples of 1.43×10^{-5} G_0 ($G_0 = 12.9$ kΩ^{-1}) with a standard deviation of $\pm 7\%$ for the peak attributed to a single molecule.[7] Later results by the same group using a similar technique on the same molecules showed two peaks associated to a single octanedithiol molecule at $7.23 \times 10^{-5} G_0$ and $2.08 \times 10^{-4} G_0$.[14] The two values are attributed to possible differences in the Au−S binding site. Using the published plots with Gaussian fits, it is possible to calculate the standard deviation for these conductance values as $\pm 16.5\%$ and $\pm 16.8\%$, respectively.

A related method was developed in which a Au scanning tunneling microscope tip is repeatedly moved into and out of contact with a Au substrate in solution containing dithiol molecules.[3] This method allows for a much greater number

* Corresponding author, dqandrews@northwestern.edu.

10.1021/nl073265l CCC: $40.75
Published on Web 03/20/2008

of measurements to be taken. The results typically show a broad peak attributed to a single molecule and higher order conductance peaks.[3,11,15–18]

These results have been extended using diamine-terminated molecules in the junction.[1,2,19,20] Tens of amine-terminated molecules have been measured, showing typical conductance variation on the order of ±40% and never showing peaks at higher multiples of conductance, attributed to multiple molecules in the junctions. The question of conductance scaling in molecular junctions is quite interesting and should be addressed in future work.[21]

Experimentally, the goal is to develop methods to control and verify single molecule junctions. Independent spectroscopic information on molecular junctions is difficult experimentally. Inelastic tunneling spectroscopy has been used to gather information on single molecule junctions, but the demanding requirements of liquid helium temperatures and exceptional stability limit its application.[22–26] Another direct method of characterizing single molecule transport junctions that should be possible is using surface-enhanced Raman scattering (SERS)[27–29] because the metal−molecule−metal junctions studied here are also analogous to structures used to generate single-molecule SERS.[30]

Theoretical approaches to charge transport through junctions have focused on the Landauer/Imry limit, of elastic scattering, calculated using a nonequilibrium Green's function (NEGF).[31] This formalism is most straightforward for calculations made in the limit of strong coupling to the electrodes and coherent transport in the low bias regime far from molecular resonances.[32] One of the simplifications nearly always used to date in molecular transport junctions is the assumption of static geometry. Several recent papers have attempted to calculate charge transport for varying molecular geometries,[33] but due to the cost of transport calculations typically only one or a few molecular orientations were used to calculated transport behavior. Past results from our group and other groups have shown that for a chemisorbed *p*-benzenedithiol molecule between Au electrodes the molecular orientation and binding site can have an effect of up to 3 orders of magnitude on the conductances.[34–37]

In a recent paper, a large force field molecular dynamics calculation was preformed on a monolayer of biphenyldithiol.[38,39] The molecular dynamics method was then used to find three packing structures that were energetically favorable for biphenyldithiol, and the transport behaviors of these three structures were calculated and compared.[40] The main results of this paper indicate that there is a relatively flat potential energy surface with respect to the tilt of the molecule above the Au surface. For two different tilt angles of 15 and 30°, the low bias conductance varied up to half an order of magnitude, attributed to changes in the sulfur−Au coupling.[40]

With most experimental measurements at room temperature, the phase space sampled by the molecule and the electrode could have a critical effect on the measured conductance. This dynamic variation is typically neglected from transport calculations. In this paper, we couple molecular dynamics simulation and charge transport calculations. This allows a computational study of the thermal fluctuation and geometric effects on conductance (Figure 1).[41]

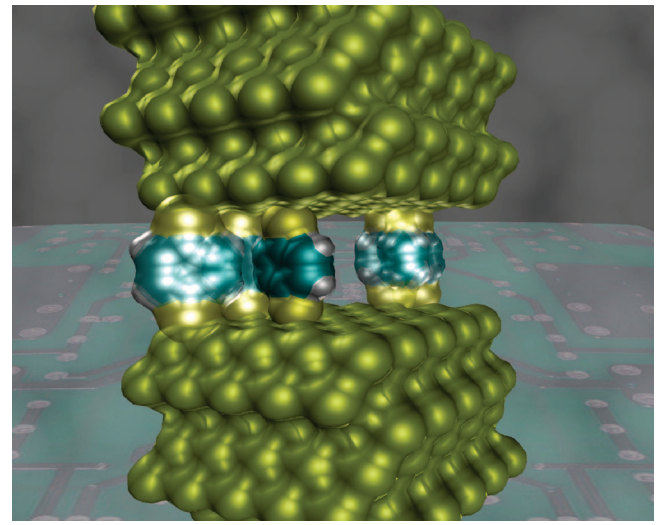

Figure 1. Simulation of a single molecule electronic device. The image shows multiple timeshots taken from a 1 ns trajectory of a dithiol-terminated molecule free to move between two Au electrodes. The slightly opaque molecules represent time steps that have already occurred but are present visually to show the dynamic nature of the Au surface−thiol interaction.

A benefit of doing molecular dynamics simulation is the ability to address the temperature dependence of molecular junction transport. This technique allows a direct calculation of the thermal width of the conductance peaks that would be expected at liquid helium and liquid nitrogen temperatures, which has not been experimentally attempted at this time.

To calculate thermal geometric fluctuations in molecular junctions, we have utilized the Tinker Molecular Dynamics program using the MM3[42–44] force field (http://dasher.wustl.edu/tinker/). The MM3 force field was modified by using the parameters calculated by Goddard et al. to describe the Au−Au and Au−organic atom interactions.[38,39] The Au metal bond interaction as used is an exponential-6 type function used to reproduce the bulk Au properties. To describe the Au−H_2N interactions, we have used the recent DFT calculations completed by Venkatarman et al. to describe the strength and distance of the Au−N bond to a single Au adatom.[2] The force field parameters otherwise used are given within the MM3 force field. A full table of all of the force field parameters used is given in the Supporting Information.

The default Au slab used in the molecular dynamics simulations was a 150 atom Au(111) pad that was six layers thick. This Au slab was coupled with periodic boundary conditions that matched the Au crystal lattice constant in the $X-Y$ plane. In the Z direction, the periodic boundary was set to 100 nm to decouple interactions between the top and bottom electrodes. In all calculations, except those noted otherwise, the Au atoms were constrained to their bulk lattice positions using a 100 kcal/(mol Å^2) harmonic force constant during the molecular dynamics simulation. The long-range Coulomb interactions were treated using the particle mesh

Ewald summation as coded in Tinker.[45] A time step of 1.0 fs was used with the Verlet algorithm to integrate the equations of motion for the system. All simulations were carried out as a canonical ensemble (NVT) using the Nose-Hoover thermostat with a relaxation time of 0.1 ps to control temperature. The suspending geometry of a molecule between two electrodes is typically a local minimum in the low coverage limit, as the molecule would preferentially lie flat on one surface.

The first step after construction of a molecular junction was minimization within Tinker using the limited-memory quasi-Newton optimization method (L-BFGS). The junction was then heated to 300 K over 50 ps. The molecular junctions were then allowed to equilibrate at 300 K for at least 500 ps. Individual junction geometric information was then recorded every picosecond for 500 ps.

For charge transport calculations, we utilized the Hückel-IV v2.0/1.0[46,47] program, a code developed at Purdue University and freely available online at Nanohub.org. The Hückel -IV program has been optimized to run with a three-atom Au pad which couples the molecule to the bulk Au electrode. To use these molecular junctions within the framework of the Hückel-IV program, the three Au atoms nearest to the S atom were parsed from the molecular dynamics simulation. In the chemisorbed *p*-benzenediamine system the three nearest Au atoms to the Au adatom were used, giving a total of four Au atoms per side. The Au adatom is needed to properly describe the Au−amine interaction.[2] An image of the *p*-benzenediamine junction is given in the Supporting Information. One assumption made in following this procedure is that there is constant coupling between the three-atom Au pad and the bulk Au electrode. Because of the relative invariance in conductance upon small variations in the Au−Au bond length, this assumption should have a minor effect on the calculated behavior.[48]

This code uses extended Hückel theory orbitals to calculate the energy of the isolated system with the three atom Au pad. There are two parameters, the Fermi level and the charging energy, U. In Hückel-IV v2.0, the energy level shift is then included through charging energy in a self-consistent field approach. In these calculations, the Fermi energy is held constant throughout the entire distribution of structures. The charging energy U is used to describe how the energy levels shift upon charge transfer to the molecule. In these calculations we have set the charging energy parameter $U = 0$. This effectively means that a change in electron transfer to the molecule will not change the energy levels of the molecule. While the charging energy for a molecule such as benzenedithiol is expected to be 1–2 eV,[49] in the low bias regime away from molecular resonance, this should not have a large effect on the conductance.[49]

First we consider a single chemisorbed *p*-benzenedithiol molecule between two 150 atom Au layers (Figure 2a). In this initial simulation, the 25 atom Au surface layers started 10.6 Å apart. The periodic boundary was matched to the Au crystal lattice in the X and Y directions. The periodic boundary in the Z direction was set to 50 nm, allowing the Au electrode slabs to vary in distance. The two-probe system was free to equilibrate for 500 ps at 300 K. The data were then collected every picosecond for the next 500 ps. The average Au−Au electrode distance was 11.07 Å as shown in the Figure 2b. Panels c and d of Figure 2 show a histogram of 500 transport calculations completed on this system. The first image is plotted on a linear−linear scale, and the second plot is shown on a log–log scale for comparison. Viewing conductance data that spans an order of magnitude or more is easiest on a log scale. To aid readability and maintain consistency between the plots all further conductance plots will be shown on a log–log scale. Supporting Information includes all plots on a linear scale. The average conductance value is $7.26 \times 10^{-3}G_0$ which compares with the published experimental result of $1.1 \times 10^{-2}G_0$.[11] In Figure 2d three molecular orientations are also shown as examples of low, average, and high conductance states of the molecule. The image representing low conductance shows the plane of the molecule intersecting one of the Au face-centered cubic (fcc) triangular faces. The high conductance state shows the plane of the molecule along one of the sides of the Au fcc triangular lattice. The average Au−S distance and the shortest Au−S bond distance showed no direct correlation to the average conductance in these three example states. This behavior was consistent through all example orientations checked. This result can be correlated to published results on symmetry breaking and conductance through the chemisorbed *p*-benzenedithiol molecule, showing increased conductance when the molecular π orbitals overlapped favorably with the Au 6s valence orbital.[36]

In the Supporting Information we have included a plot showing the transmission as a function of energy for the first 50 molecular geometries and an associated plot of the transmission variation as a function of energy. These plots show that the variation in conductance is relatively constant within the HOMO–LUMO gap but would increase if the Fermi energy was in close proximity to a molecular resonance.

The Au−Au electrode distance was then varied between 10 and 12.2 Å. In these calculations the Au atoms were all confined to their bulk lattice positions through a harmonic force constant of 100 kcal/(mol Å^2). Gaussian fits to each histogram of results using a bin size of $1 \times 10^{-4}G_0$ or $1 \times 10^{-5}G_0$ are shown in Figure 3. A comparison of a Gaussian fit and a Lorentz fit is shown in the Supporting Information. The height of the peaks is related to the bin size with lower current values giving higher peak heights. Over the 1.5 nm that the Au electrodes are separated, the average conductance value decreases more than 1 order of magnitude.

While most of the current break junction measurements have been completed at room temperature, it is important to examine what variance in conductance could be expected for a molecular junction at lower temperatures. In Figure 4 we show the change in conductance for the chemisorbed *p*-benzenedithiol system without harmonically restrained Au atoms. Five hundred conductance spectra are calculated at liquid helium temperature (4.2 K), liquid nitrogen temperature (77 K), and at 230 K along with the results for 300 K previously shown in Figure 3. The standard deviation in the

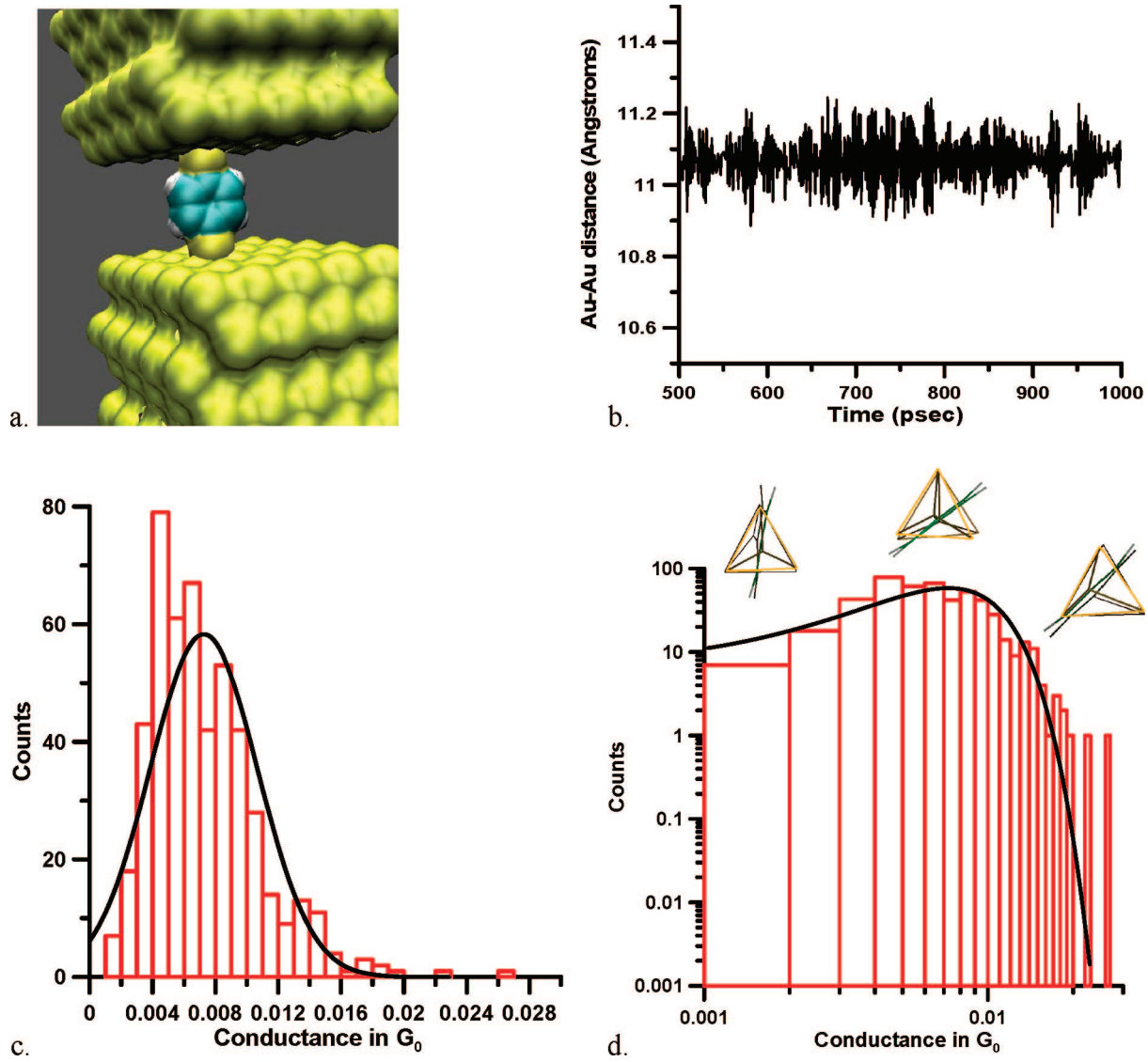

Figure 2. (a) The conductance of a chemisorbed *p*-benzenedithiol molecule between Au electrodes. The Au−Au electrode distance is free to vary as shown in (b). A histogram was calculated from 500 discrete geometries corresponding to 500 ps of molecular dynamics simulations. The bin size of both the histograms is $1 \times 10^{-3}G_0$. (c) is a linear scale and (d) shows the identical data on a log–log scale. Using a Gaussian fit the average conductance is$7.26 \times 10^{-3}G_0$ and the standard deviation is 47%. The most probable conductance value is $5 \times 10^{-3}G_0$. The insets in (d) show a top-down view of the molecular junction for three typical structures representing low, medium, and high conductance.

conductance decreases from 47% at room temperature to 22.2% at liquid nitrogen temperature to 6.6% at liquid helium temperature. The mean conductance value also decreases from $0.0112G_0$ at 300 K to $0.007G_0$ at 4.2 K. This value is very similar to the most probable conductance value of $0.008G_0$ calculated at 300 K.

To compare with other recent experimental results we have also calculated the conductance variation that can be expected for a chemisorbed *p*-benzenediamine molecule between two Au electrodes. The amine Au interaction is weaker than the Au−sulfur interaction, and it is expected that an amine-terminated molecule interacts only with a Au adatom on the surface.[2] In order to model this, we have used a Au adatom that is free to move in our molecular dynamics and transport calculations for the amine-terminated molecules. The bulk Au electrode atoms remain harmonically fixed. Figure 5 shows the distribution in conductance values for 100 geometries from 100 ps of simulation for a fixed Au−Au electrode distance of 11.0 Å. The average conductance value is $0.012G_0$, and the standard deviation is 37%. At an electrode distance of 11.0 Å, this standard deviation is a bit lower than that calculated for the chemisorbed *p*-benzenedithiol system (47%) shown in Figure 1. While the average conductance is quite similar to that calculated for the chemisorbed *p*-benzenedithiol molecule, we remind the reader that the Fermi energy is an adjustable parameter in these Hückel IV calculations and a small shift in the Fermi energy toward or away from the highest occupied orbital resonance could have a large effect on the magnitude of the conductance.

To test the change in conductance with the change in electrode distance, we varied the electrode distance and calculated the transport values. Figure 6 shows the Gaussian fits for 100 geometries at 10, 11, 12, and 13 Å electrode

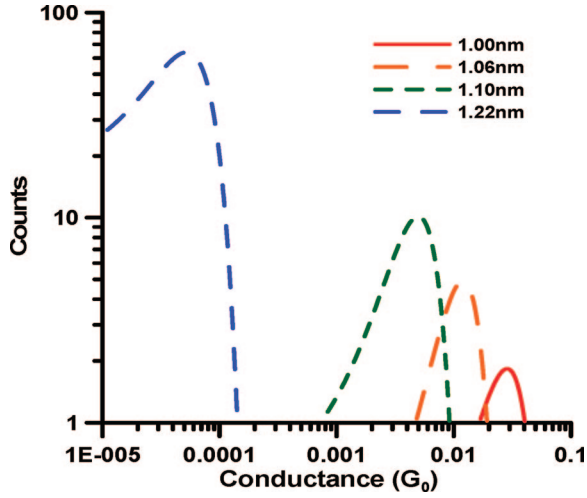

Figure 3. Gaussian curves fit to 500 geometries for a chemisorbed *p*-benzendithiol molecule between to Au electrodes. The Au atoms are fixed in each simulation and between simulations the electrode separation is varied from 10 to 12.2 Å. The height of the peaks is related to both the standard deviation in conductance and to the histogram bin width, which is $1 \times 10^{-5}G_0$ for 12.2 Å and $1 \times 10^{-4}G_0$ for 10, 10.6, and 11 Å separation.

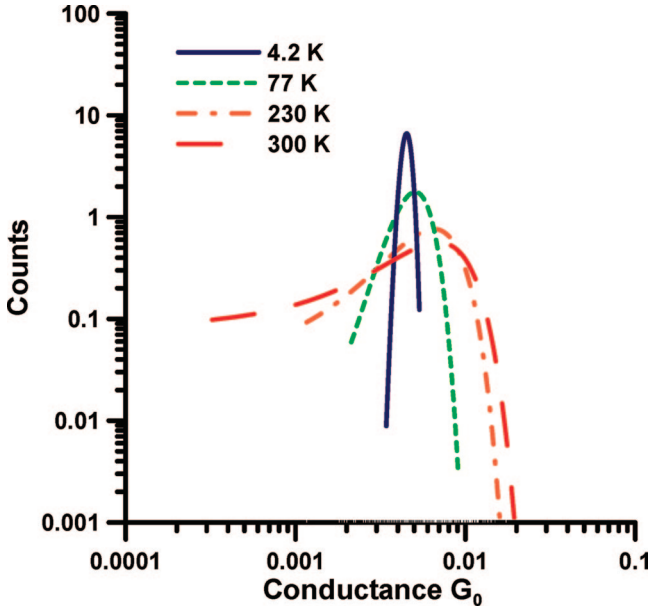

Figure 4. Temperature dependence for a Au-chemisorbed *p*-benzendithiol−Au junction. The Au electrodes were free to move in the *Z* direction but stayed on average 11.05 Å apart. The standard deviation decreases from 47% at 300 K to 6.6% at 4.2 K.

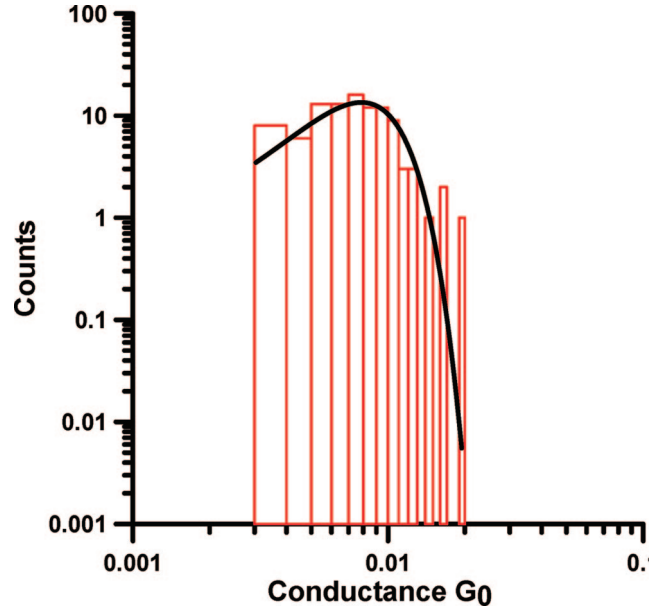

Figure 5. A chemisorbed *p*-benzenediamine molecule between Au electrodes at a fixed separation distance of 11 Å. The molecular junction was equilibrated for 900 ps and then every picosecond for 100 ps a geometry was taken and the transport behavior was calculated. The red bar graph shows a histogram of the conductance with a bin size of $0.01G_0$ while the black line shows a Gaussian fit to the data. The average conductance is $7.8 \times 10^{-3}G_0 \pm 37\%$.

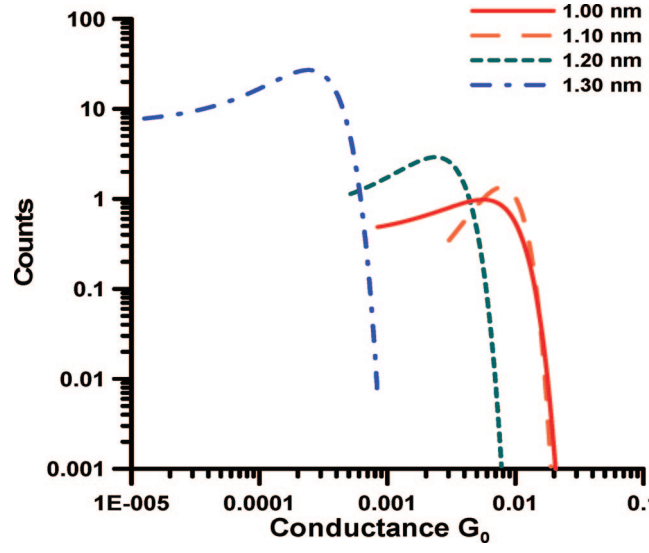

Figure 6. A chemisorbed *p*-benzenediamine molecule between Au electrodes at a varied Au electrode distance. A Gaussian fit for 100 geometries from 100 ps of simulation are shown. The histogram bin size is held constant at $1 \times 10^{-4}G_0$.

separation distance. It should be noted that the peaks in the fit for 10, 11, and 12 Å are quite close together. To compare to the chemisorbed *p*-benzenedithiol molecule, Figure 7a shows a plot of the average values and the standard deviations upon electrode separation. In the plot it should be noted that the Au−S conductance seems to decrease rapidly upon electrode separation while the Au−amine conductance has a much slower rate of initial change in conductance. For both molecular systems the electrode separation corresponding to the minimum energy also has the smallest deviation in conductance values. The comparison with the published experimental results is shown in Figure 7b. Both the peak position and the distribution of calculated values show good agreement.

The results presented here mirror single molecule experimental results in showing a wide distribution of current values attributed to a single molecule junction. Our results show similar deviation in conductance values and assumed a chemisorbed *p*-benzenedithiol molecule on a Au surface and a chemisorbed *p*-benzenediamine molecule bound to a free Au adatom on a Au surface. The chemisorbed *p*-

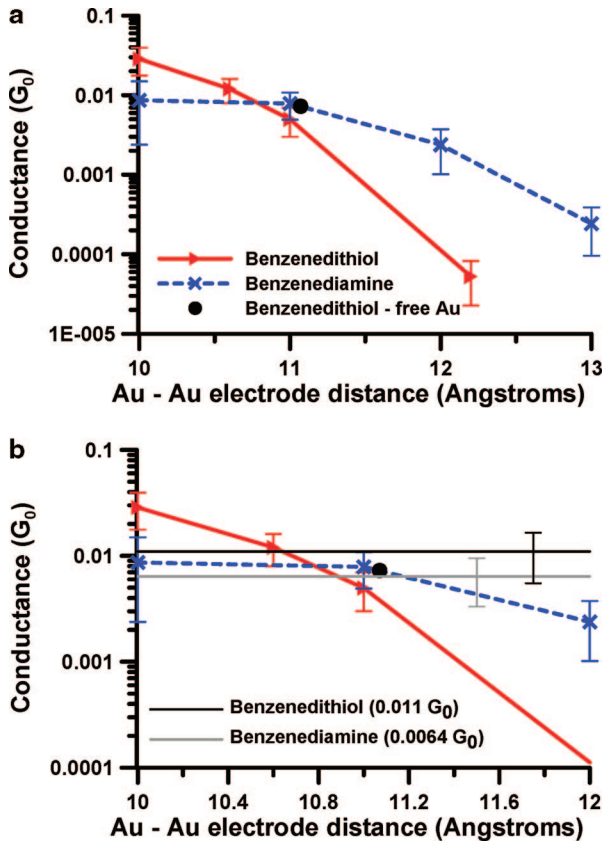

Figure 7. (a) Conductance vs electrode−electrode distance for both the chemisorbed *p*-benzenedithiol and the chemisorbed *p*-benzenediamine molecules. (b) The calculated results from Figure 7a plotted with published experimental results (black and gray lines) for the conductance through the chemisorbed *p*-benzenedithiol and the chemisorbed *p*-benzenediamine molecules.[2,11] The error bars on the experimental lines are approximated from the published figures and, since the measurements are not associated with an electrode distance, only placed on the graph to aid in comparison with our results.

benzenediamine molecule conductance varied little upon stretching the interelectrode distance by 2 Å. This can be compared to the chemisorbed *p*-benzenedithiol molecule, which showed a rapid decrease in conductance with increasing electrode distance. These results seem to indicate that building single molecule electronic devices with reproducible conductance at room temperature using Au electrodes with sulfur or amine coupling will be extremely difficult due to the large variances arising from thermal fluctuations.

Concerning the accuracy of these calculations, there are three main considerations: the description and geometry of a molecular junction, the accuracy of the molecular dynamics force field, and the adequacy of the transport code. Our description of the junction geometry is simplified by having two matching fcc-terminated Au electrodes with a molecule bridging the gap. In the room temperature scanning probe electrochemical break junction experiments, the repeated motion of bringing a Au tip into contact with a Au surface likely creates disordered electrodes. Upon retraction of the Au tip, it is also quite likely that a Au neck forms and that this Au neck is more likely to break than the Au−S bond.[11,50] Attempting to model accurately a Au tip may be important for a comparison with experiment, but as a first approximation we have focused on using two defined electrodes.

The Au−Au and the Au−molecule force field potentials have not been extensively tested in the literature. There is a high cost of performing calculations on the large number of Au atoms required to describe the surface and the surface molecule interactions. In the static limit there have been a number of papers describing the location of a sulfur bound molecule above the Au surface (for more detail see ref 51). While the Au−S interaction is greatly oversimplified by using the exp-6 function in the molecular dynamics, we do not believe that this greatly changes our results on the distribution of geometries and current values that might be measured in a single molecule junction.

In terms of charge transport codes, we have used a robust, well-tested code using extended Hückel molecular orbitals. This code has been shown to have results qualitatively equivalent to computationally more expensive DFT-based codes.[46,48,49,52] The importance of the treatment of the electrostatic potential increases with increasing voltage; therefore we have limited our results to the low bias regime, specifically conductance at 20 mV. This voltage bias corresponds well with experimental methods[1,3,11,19]

A recent paper computationally addresses the issue of amine and thiol terminal groups in break junction experiments utilizing DFT methods to optimize the structure at various electrode distances.[53] Their results, in contrast to ours, show a quick drop off in the amine-terminated conductance, whereas the chemisorbed *p*-benzendithiol molecules show a large rise in conductance before decreasing with increasing electrode distance.[53] This is due to a calculated charge transfer to the molecule and the use of self-consistent-field methods and a first-principles Hamiltonian for the molecule.[17,48,54–57] Another recent paper, which computes the conductance of 15 distinct Au−*p*-benzenediamine geometries using a DFT code, calculates a distribution of conductance values similar to the experimental results, but an average conductance value seven times higher.[58] Our method seems to provide a reasonable comparison with experimental results, capturing the dynamics of a charge transport junction and the associated current fluctuations.

Using molecular dynamics and an extended Hückel nonequilibrium Green's function transport code, we have modeled transport junctions. We find good agreement with experimental measurements with respect to both the magnitude and width of the measured conductance peaks. This technique of modeling a transport junction as an ensemble of molecular geometries gives insight into how the thermal fluctuations of a junction can provide a large distribution of conductance values. This technique could be valuable in the design and understanding of single molecule junctions with reproducible conductance.

Acknowledgment. We thank ATOMISTIX for access to the ATK program and Gemma Solomon for helpful discussion. This work was supported by the National Science Foundation through Grants EEC-0228390 and CHE0414554 (Network for Computational Nanotechnology) and CHE-

0719420, and by the NSF-MRSEC program through the Northwestern MRSEC, by the DOD MURI program, and the NASA-URETI program.

Supporting Information Available: Figures showing the chemisorbed *p*-benzenediamine junction, variations in transmission as a function of energy, Gaussian fitting, plots with a linear current axis, and a view of the Au surface potential and a table of force field parameters. This material is available free of charge via the Internet at http://pubs.acs.org.

References

(1) Venkataraman, L.; Klare, J. E.; Nuckolls, C.; Hybertsen, M. S.; Steigerwald, M. L. *Nature* **2006**, *442* (7105), 904–907.
(2) Venkataraman, L.; Klare, J. E.; Tam, I. W.; Nuckolls, C.; Hybertsen, M. S.; Steigerwald, M. L. *Nano Lett.* **2006**, *6* (3), 458–462.
(3) Xu, B.; Tao, N, J. *Science* **2003**, *301(* (5637), 1221–1223.
(4) Aviram, A.; Ratner, M. A. *Chem. Phys. Lett.* **1974**, *29* (2), 277–283.
(5) Emberly, E. G.; Kirczenow, G. *Phys. Rev. Lett.* **2003**, *91* (18), 188301.
(6) Cardamone, D. M.; Stafford, C. A.; Mazumdar, S. *Nano Lett.* **2006**, *6* (11), 2422–2426.
(7) Cui, X. D.; Primak, A.; Zarate, X.; Tomfohr, J.; Sankey, O. F.; Moore, A. L.; Moore, T. A.; Gust, D.; Harris, G.; Lindsay, S. M. *Science* **2001**, *294* (5542), 571–574.
(8) Reed, M. A.; Zhou, C.; Muller, C. J.; Burgin, T. P.; Tour, J. M. *Science* **1997**, *278* (5336), 252–254.
(9) Smit, R. H. M.; Noat, Y.; Untiedt, C.; Lang, N. D.; van Hemert, M. C.; van Ruitenbeek, J. M. *Nature* **2002**, *419* (6910), 906–909.
(10) Kiguchi, M.; Stadler, R.; Kristensen, I. S.; Djukic, D.; Ruitenbeek, J. M. v *Phys. Rev. Lett.* **2007**, *98* (14), 146802.
(11) Xiao, X.; Xu, B.; Tao, N. J. *Nano Lett.* **2004**, *4* (2), 267–271.
(12) Suzuki, M.; Fujii, S.; Fujihira, M. *Jpn. J. Appl. Phys.* **2006**, *45* (3B), 2041–2044.
(13) Chen, F.; Hihath, J.; Huang, Z.; Li, X.; Tao, N. J. *Annu. Rev. Phys. Chem.* **2007**, *58*, 535–564.
(14) Morita, T.; Lindsay, S. *J. Am. Chem. Soc.* **2007**, *129*, 7262–7263.
(15) Ke, S.-H.; Baranger, H. U.; Yang, W. *J. Am. Chem. Soc.* **2004**, *126* (48), 15897–15904.
(16) Li, X. L.; He, H. X.; Xu, B. Q.; Xiao, X. Y.; Nagahara, L. A.; Amlani, I.; Tsui, R.; Tao, N. J. *Surf. Sci.* **2004**, *573* (1), 1–10.
(17) Ke, S.-H.; Baranger, H. U.; Yang, W. *J. Chem. Phys.* **2005**, *122* (7), 074704.
(18) Chen, F.; Hihath, J.; Huang, Z.; Li, X.; Tao, N. J. *Annu. Rev. Phys. Chem.* **2007**, *58* (1), 535–564.
(19) Venkataraman, L.; Park, Y. S.; Whalley, A. C.; Nuckolls, C.; Hybertsen, M. S.; Steigerwald, M. L. *Nano Lett.* **2007**, *7* (2), 502–506.
(20) Ulrich, J.; Esrail, D.; Pontius, W.; Venkataraman, L.; Millar, D.; Doerrer, L. H. *J. Phys. Chem. B* **2006**, *110* (6), 2462–2466.
(21) Landau, A; Kronik, L.; Nitzan, A. *Condens. Matter* **2007**, arXiv: 0707.3038.
(22) Stipe, B. C.; Rezaei, M. A.; Ho, W. *Science* **1998**, *280* (5370), 1732–1735.
(23) Kushmerick, J. G.; Allara, D. L.; Mallouk, T. E.; Mayer, T. S. *MRS Bull.* **2004**, *29* (6), 396–402.
(24) Troisi, A.; Beebe, J. M.; Picraux, L. B.; van Zee, R. D.; Stewart, D. R.; Ratner, M. A.; Kushmerick, J. G. *Proc. Natl. Acad. Sci. U.S.A.* **2007**, *104* (36), 14255–14259.
(25) Hahn, J. R.; Lee, H. J.; Ho, W. *Phys. Rev. Lett.* **2000**, *85* (9), 1914.
(26) Wang, W.; Lee, T.; Kretzschmar, I.; Reed, M. A. *Nano Lett.* **2004**, *4* (4), 643–646.
(27) Ward, D. R.; Grady, N. K.; Levin, C. S.; Halas, N. J.; Wu, Y.; Nordlander, P.; Natelson, D. *Nano Lett.* **2007**, *7* (5), 1396–1400.
(28) Domke, K. F.; Zhang, D.; Pettinger, B. *J. Am. Chem. Soc.* **2006**, *128* (45), 14721–14727.
(29) Tian, J. H.; Liu, B.; Li, X. L.; Yang, Z. L.; Ren, B.; Wu, S. T.; Tao, N. J.; Tian, Z. Q. *J. Am. Chem. Soc.* **2006**, *128* (46), 14748–14749.
(30) Dieringer, J. A.; Lettan, R. B.; Scheidt, K. A.; Van Duyne, R. P. *J. Am. Chem. Soc.* **2007**, .
(31) Landauer, R. *J. Phys.: Condens. Matter* **1989**, *1*, 8099–81100.
(32) Datta, S., *Quantum Transport: Atom to Transistor*; Cambridge University Press: Cambridge,2005.
(33) Hu, Y.; Zhu, Y.; Gao, H.; Guo, H. *Phys. Rev. Lett.* **2005**, *95* (15), 156803–4.
(34) Geng, W. T.; Jun, N.; Takahisa, O. *Appl. Phys. Lett.* **2004**, *85* (24), 5992–5994.
(35) Hu, W.; Jiang, J.; Nakashima, H.; Luo, Y.; Kashimura, Y.; Chen, K.-Q.; Shuai, Z.; Furukawa, K.; Lu, W.; Liu, Y.; Zhu, D.; Torimitsu, K. *Phys. Rev. Lett.* **2006**, *96* (2), 027801-4.
(36) Basch, H.; Cohen, R.; Ratner, M. A. *Nano Lett.* **2005**, *5* (9), 1668–1675.
(37) Solomon, G. C.; Reimers, J. R.; Hush, N. S. *J. Chem. Phys.* **2005**, *122* (22), 224502.
(38) Jang, Y. H.; Jang, S. S.; Goddard, W. A. *J. Am. Chem. Soc.* **2005**, *127* (13), 4959–4964.
(39) Jang, S. S.; Jang, Y. H.; Kim, Y. H.; Goddard, W. A.; Flood, A. H.; Laursen, B. W.; Tseng, H. R.; Stoddart, J. F.; Jeppesen, J. O.; Choi, J. W.; Steuerman, D. W.; DeIonno, E.; Heath, J. R. *J. Am. Chem. Soc.* **2005**, *127* (5), 1563–1575.
(40) Yong-Hoon, K.; Seung Soon Jang William, A. G. *J. Chem. Phys.* **2005**, *122* (24), 244703. Iii. .
(41) Humphrey, W.; Dalke, A.; Schulten, K. *J. Mol. Graphics* **1996**, *14*, 33–38.
(42) Allinger, N. L.; Yuh, Y. H.; Lii, J. H. *J. Am. Chem. Soc.* **1989**, *111* (23), 8551–8566.
(43) Lii, J. H.; Allinger, N. L. *J. Am. Chem. Soc.* **1989**, *111* (23), 8566–8575.
(44) Lii, J. H.; Allinger, N. L. *J. Am. Chem. Soc.* **1989**, *111* (23), 8576–8582.
(45) Ponder, J. W. *Tinker*,4.2; Washington University School of Medicine, 2004.
(46) Tian, W.; Datta, S.; Hong, S.; Reifenberger, R.; Henderson, J. I.; Kubiak, C. P. *J. Chem. Phys.* **1998**, *109* (7), 2874–2882.
(47) ZahidF. PaulssonM. DattaS. Electrical Conduction through Molecules. In *Advanced Semiconductors and Organic Nano-Techniques*; Morkoc, H., Ed.; Academic Press: New York, 2003; Vol. 3, pp 1−41.
(48) Andrews, D. Q.; Cohen, R.; Van Duyne, R. P.; Ratner, M. A. *J. Chem. Phys.* **2006**, *125* (17), 174718.
(49) Zahid, F.; Paulsson, M.; Datta, S., Electrical Conduction through Molecules. In *Advanced Semiconductors and Organic Nano-Techniques Part III: Physics and Technology of Molecular and Biotech Systems*, Morkoc, H. , Ed. Elsevier Academic Press: San Diego, CA, 2003; Vol. III, pp 1–40.
(50) Krüger, D.; Fuchs, H.; Rousseau, R.; Marx, D.; Parrinello, M. *Phys. Rev. Lett.* **2002**, *89* (18), 186402.
(51) Bilic, A.; Reimers, J. R.; Hush, N. S. *J. Chem. Phys.* **2005**, *122* (9), 094708.
(52) Zahid, F.; Ghosh, A. W.; Paulsson, M.; Polizzi, E.; Datta, S. *Phys. Rev. B: Condens. Matter Mater. Phys.* **2004**, *70* (24), 245317/1–245317/5.
(53) Zhenyu, L.; Kosov, D. S. *Phys. Rev. B: Condens. Matter Mater. Phys.* **2007**, *76* (3), 035415.
(54) Xue, Y.; Ratner, M. A. *Phys. Rev. B: Condens. Matter Mater. Phys.* **2003**, *68* (11), 115406/1–115406/18.
(55) Xue, Y.; Ratner, M. A. *Phys. Rev. B: Condens. Matter Mater. Phys.* **2003**, *68* (11), 115407/1–115407/11.
(56) García-Suárez, V. M.; Kostyrko, T.; Bailey, S.; Lambert, C.; Bulka, B. R. *Phys. Status Solidi B* **2007**, *244* (7), 2443–2447.
(57) Romaner, L.; Heimel, G.; Gruber, M.; Brédas, J.-L.; Zojer, E. *Small* **2006**, *2* (12), 1468–1475.
(58) Quek, S. Y.; Venkataraman, L.; Choi, H. J.; Louie, S. G.; Hybertsen, M. S.; Neaton, J. B. *Nano Lett.* **2007**, *7* (11), 3477–3482.

NL073265L